A high-throughput whole cell screen to identify inhibitors of *Mycobacterium tuberculosis*

Juliane Ollinger, Anuradha Kumar, David M. Roberts, Mai A. Bailey, Allen Casey and Tanya Parish*

Infectious Disease Research Institute, 1616 Eastlake Avenue E, Suite 400, Seattle, Washington 98102

Running title

M. tuberculosis whole cell screen

Key Words

Mycobacterium tuberculosis, fluorescent proteins, drug discovery, high throughput assay, anti-tubercular

Declarations of interest: none

Corresponding author

Tanya Parish

Tanya.Parish@idri.org

ABSTRACT

Tuberculosis is a disease of global importance for which novel drugs are urgently required. We developed a whole-cell phenotypic screen which can be used to identify inhibitors of *Mycobacterium tuberculosis* growth. We used recombinant strains of virulent *M. tuberculosis* which express far-red fluorescent reporters and used fluorescence to monitor growth *in vitro*. We optimized our high throughput assays using both 96-well and 384-well plates; both formats gave assays which met stringent reproducibility and robustness tests. We screened a compound set of 1105 chemically diverse compounds previously shown to be active against *M. tuberculosis* and identified primary hits which showed ≥ 90% growth inhibition. We ranked hits and identified three chemical classes of interest – the phenoxyalkylbenzamidazoles, the benzothiophene 1-1 dioxides, and the piperidinamines. These new compound classes may serve as starting points for the development of new series of inhibitors that prevent the growth of *M. tuberculosis.* This assay can be used for further screening, or could easily be adapted to other strains of *M. tuberculosis.*

INTRODUCTION

Tuberculosis (TB), caused by the bacterial pathogen *Mycobacterium tuberculosis*, is a disease of global importance which killed approximately 1.7 million people in 2016 (1). A lengthy 4-drug regimen is used to treat active infection, but drug resistant strains have emerged and threaten efforts to control the disease. Multi-drug resistant (MDR) and extremely drug resistant (XDR) TB are gaining footholds in areas where HIV is predominant and/or antibiotic treatment of patients is administered incompletely or incorrectly (1). Thus, there is an urgent need for new drugs that are effective at killing *M. tuberculosis* and which might shorten therapy.

High throughput screening of small molecules has the potential to identify new compound classes that are effective against *M. tuberculosis*. Biochemical screens have been used to find inhibitors of specific targets, normally essential enzymes. A number of targets have been tested (2-15) but this approach had limited success in finding hits with whole cell activity for a variety of reasons including lack of permeation, efflux, and poor target vulnerability or engagement (16).

In contrast, phenotypic screening relies on identifying compounds with whole cell activity from the outset, with no knowledge of the cellular target. Although there remain challenges in dealing with an organism which grows very slowly and requires handling within specialized containment facilities. A number of assays have been developed which use different approaches, for example the use of non-pathogenic surrogates such as

Mycobacterium tuberculosis H37Ra (17), *Mycobacterium smegmatis* (18) or *Mycobacterium aurum* (19). High throughput screening has been conducted with *M. tuberculosis* under a variety of conditions, including nutrient starvation (20), under multiple stresses (21, 22), or during infection of host cells (23, 24). Assays using live cells are also available to determine disruption of specific pathways, such as ATP homeostasis (25), pH homeostasis (26), biofilm formation (27) or under specific conditions such as low oxygen (28).

MATERIAL AND METHODS

Bacterial strains and growth conditions

M. tuberculosis H37Rv LP (ATCC 25618) (29) was grown in Middlebrook 7H9 medium supplemented with 10% v/v oleic acid, albumin, dextrose, catalase (OADC; Becton Dickinson), 0.05% w/v Tween 80 (7H9-OADC-Tw), and 50 µg/mL hygromycin (7H9-OADC-Tw-hyg), where required. Large scale cultures were grown in 100 mL of medium in 450 cm^2 roller bottles at 37^oC and 100 rpm. *M. tuberculosis* strain CHEAM3 and DREAM8 expressing codon-optimized mCherry and *Ds*Red from plasmids pCherry3 (30) and pBlazeC8 (31), respectively, were used.

Preparation of assay plates

Medium and compound was dispensed into sterile, black, 384-well, clear bottom plates (Greiner) using a Minitrak (Packard BioScience) with a 384-well head contained in a custom HEPA enclosure. Controls were 100 µM rifampicin in column 1 (final assay concentration of 2 µM rifampicin), DMSO in column 2 (final assay concentration 2%) and

84 125 nM rifampicin in column 23 (final assay concentration of 2.5 nM). *M. tuberculosis*
85 culture was added to columns 1-23 using a MultiDrop Combi (Thermo Fisher); column 24
86 was not inoculated (contamination control).
87
88 **Growth in plates**
89 *M. tuberculosis* was grown to logarithmic phase (OD_{590} = 0.6-0.9) and filtered through a
90 0.5 µm cellulose-acetate membrane filter, diluted in fresh medium, and inoculated into
91 96-well or 384-well plates containing medium. Plates were incubated in plastic bags in a
92 humidified incubator at 37°C. OD and fluorescence were read using a Synergy 4 plate
93 reader (BioTek) with excitation/emission of 586nm/614nm for mCherry and
94 560nm/590nm for *Ds*Red.
95
96 **Data Analysis**
97 OD_{590} and fluorescence readouts were analyzed independently. The coefficient of
98 variation (CV) was calculated as the standard deviation (StdDev) ÷ Mean. For each plate
99 the minimum and maximum growth controls were used to determine the signal to
100 background (S:B) ratio (calculated as MeanMaxSignal ÷ MeanMinSignal), signal to noise
101 (S:N) ratio (calculated as (MeanMaxSignal-MeanMinSignal) ÷ StdDevMinSignal), and
102 the Z' of the controls (1-((3*StdDevMaxSignal+3*StdDevMinSignal) ÷ (MeanMaxSignal-
103 MeanMinSignal)). For each well, the % inhibition was calculated with reference to the
104 maximum growth control (DMSO only).
105
106 The complete data set is available at

https://pubchem.ncbi.nlm.nih.gov/bioassay/1259417?viewcode=51D85DCA-C8B4-48D9-B4BE-37687D75149B

RESULTS AND DISCUSSION

Assay development

We were interested in developing a simple whole cell screen which could be used in multiple formats to assess the anti-tubercular activity of large compound sets. We previously developed an assay to monitor growth based on fluorescence and optical density using a strain of *M. tuberculosis* constitutively expressing the far-red reporter mCherry which was robust and reproducible in 96-well format (32). In this study we used recombinant *M. tuberculosis* constitutively expressing either codon-optimized *Ds*Red or mCherry to develop a 384-well high throughput assay.

We determined the minimum inhibitory concentration (MIC) for rifampicin against the parental strain (H37Rv-LP; ATCC 25618) and both the fluorescent strains (CHEAM3 expressing mCherry from plasmid pCherry3, and DREAM8 expressing *Ds*Red from plasmid pBlazeC8). We used a 10-point, 2-fold serial dilution in independent experiments in 96-well plates. Growth inhibition was calculated compared to control wells (DMSO), and curves fit using the Levenberg-Marqardt algorithm. For both strains, we calculated MICs using OD_{590} and fluorescence independently and observed that the MIC for rifampicin was equivalent to the parental strain H37Rv-LP strain (Table 1). MICs derived using fluorescence as a readout were equivalent to OD_{590}-derived values (Table 1). Once

we had confirmed the equivalence of the three strains in 96-well plates, we determined key parameters for transferring the assay to higher throughput in 384-well plates.

Table 1. Determination of rifampicin activity against recombinant strains

	MIC (μM)	
	(OD_{590})	(RFU)
H37Rv-LP	6.6 ± 2.5 (n=85)	*na*
CHEAM3	7.5 ± 1.9 (n=96)	6.8 ± 2.2 (n=86)
DREAM8	7.1 ± 2.2 (n=520)	6.9 ± 2.4 (n=520)

MIC, the concentration required to inhibit growth by 90%; *na,* not applicable

Optimizing fluorescence measurements

We optimized a number of parameters and variables. We had previously determined the optimal parameters for measuring mCherry fluorescence (32). For *Ds*Red, we ran a set of spectral scans varying the excitation wavelength from 540 nm to 565 nm with a fixed emission of 590 nm, and varying the emission wavelength from 580 to 630 nm with a fixed excitation of 558 nm (Figs 1A and B). The signal was optimal at a range of excitation wavelengths around 560 nm, while it peaked at the emission wavelength of 592nm. Based on these scans we selected excitation and emission wavelengths of 560nm and 590nm for *Ds*Red.

Fig 1. Optimization of fluorescence measurements. DREAM8 was dispensed into 384-well plates and fluorescence was measured at varying excitation wavelengths when the emission wavelength was fixed at 590nm (A) or at varying emission wavelengths when a fixed excitation of 558nm was used (B). Data are the average ± SD from four wells.

We tested the alternatives of bottom and top-read optics in the plate-reader. We compared the use of an external plate shaker or the integral plate shaker in the reader. We obtained the lowest signal to noise (S:N) ratio when plates were not shaken prior to reading and when fluorescence measurements were performed using the bottom optics on the plate reader (data not shown).

Optimizing inoculum and growth conditions

Several additional assay parameters were tested in the 384-well plates to determine the final assay conditions; the inoculum concentration, and the number of days of incubation prior to measurement of *M. tuberculosis* growth were adjusted to minimize the assay volume while optimizing for signal and reproducibility. At a starting OD_{590} of 0.01, growth was still logarithmic between 4 and 5 days of incubation, whereas at a higher inoculum of OD_{590} = 0.05, cell growth plateaued at 5 days of growth (data not shown). To refine further we performed serial dilutions of CHEAM3 and monitored growth after five days of incubation. We measured fluorescence at the start of the experiment and on day 5 and calculated the S:B ratio (using the values obtained on day 0 of the experiment as the background) (Fig 2A). Wells with starting densities of 0.02 - 0.03 gave the highest S:B (Fig 2A). We ran a similar experiment using starting inocula of 0.01, 0.02 and 0.03 and incubated for 4 or 5 days, but we measured the ratio between full growth and complete inhibition using 2 µM rifampicin (Fig 2B); we found a higher ratio using OD_{590} of 0.02-0.03 (ratio of 13.0 and 13.8 respectively). However, variation was greater using the larger inoculum of OD_{590}=0.03, with a coeffeicient of variance (CV) of 9%, as compared to a CV

of 5% for the inoculum at OD_{590}=0.02. Thus a starting OD_{590} of 0.02 produced the best signal window and reproducibility in the 384-well assay.

Fig 2. Optimization of growth conditions. (A) Serial dilutions of CHEAM3 were plated in triplicate in a 384 well plate and measured for fluorescence before and after five days of incubation. The signal to background (S:B) for each inoculum was calculated (average signal D0÷average signal D5) to identify the greatest amplitude to measure growth of cells over the course of 5 days. (B) 320 experimental wells of a 384 well plate were inoculated with CHEAM3 diluted to a starting OD_{590} of 0.01, 0.02 or 0.03. Plates were read on D4 and D5. The average fluorescence for each condition (n=320) was plotted, with error bars indicating the standard deviation. The calculated signal to background (S:B) is shown above each bar.

Our final assay conditions were to inoculate 10 µL of *M. tuberculosis* at OD_{590} = 0.06 into 384-well plates prefilled with 20 µL of medium to give a final theoretical OD_{590} of 0.02. Plates were incubated for 5 days at 37°C and both fluorescence and OD_{590} measured.

Validation of 384-Well Plate Assay

Once the assay conditions were optimized, we assessed reproducibility according to NCGC guidelines (33). Assay plates containing 20 µL of 7H9-Tw-OADC medium were prepared in a sterile environment. For validation, DMSO or test compounds were added to wells and the plates were inoculated with 10 µL of *M. tuberculosis* at an OD_{590} of 0.06. The final volume in each well was 30 µL, the final OD_{590} was 0.02, and the final concentration of DMSO in each well was 2%. Plates were incubated for five days at 37°C in a humidified incubator. The plate layout was arranged as 320 sample wells in columns

3-22. The remaining four columns were reserved for plate controls: Column 1 - minimum signal (2 μM rifampicin); Column 2 - maximum signal (DMSO); Column 23 - midpoint signal (2.5 nM rifampicin); Column 24 – contamination control (medium only, no inoculum). To test assay reproducibility, we ran a set of six plates independently on three days; two plates of minimum signal, two plates, of maximum signal and two plates of midpoint signal (Fig 3). The % growth in each well was calculated with reference to the maximum signal (Column 2).

Fig 3. High throughput screen validation scatter plots: Two plates each of containing minimum, midpoint, and maximum signal controls were run in 384-well plates on three separate days using the final assay conditions. Recombinant *M. tuberculosis* expressing (A) *Ds*Red or (B) mCherry was grown for 5 days. Relative fluorescence units (RFU) were measured in each well.

For each strain 2 plates containing maximum signal (Max = *M. tuberculosis* grown with 2% DMSO), mid signal (Mid = *M. tuberculosis* grown in the presence of 2.5 nM rifampicin), and minimum signal (Min = *M. tuberculosis* in the presence of 2 μM rifampicin) were run on three separate days. Max and Min controls (n=16) from within each plate were used to calculate the signal to noise ratio (S:N), signal to backround ratio (S:B), and Z' factor (measure of assay robustness as defined earlier). Intraplate controls were also used to calculate the % growth in each well. For the 320 sample wells in each individual plate the average signal, percent coefficient of variance (% CV) of the signal, and average % growth were calculated. The assay statistics generated to validate these two high throughput screens are shown in Tables 2A and B.

218 **Table 2. High throughput screen validation statistics.**

A. DREAM8 validation

intra-plate controls

Signal	Day	Plate	S:N	S:B	Z '	Avg Signal (RFU)	% CV	% growth
Max	1	1	169	13	0.90	12.8	6.9	-0.4
Max	1	2	261	13	0.89	12.8	6.5	-0.4
Max	2	1	189	14	0.93	13.0	8.4	-0.1
Max	2	2	127	14	0.91	13.4	7.8	0.3
Max	3	1	119	14	0.87	12.5	7.8	0.0
Max	3	2	187	15	0.83	12.3	7.4	0.1
Mid	1	1	179	13	0.89	110.6	6.4	60.7
Mid	1	2	250	13	0.88	105.1	4.7	58.3
Mid	2	1	244	12	0.93	135.8	3.3	79.2
Mid	2	2	106	12	0.92	132.8	3.2	78.4
Mid	3	1	226	14	0.90	126.1	7.8	69.8
Mid	3	2	187	14	0.87	121.4	5.2	68.0
Min	1	1	178	13	0.88	161.2	2.1	97.3
Min	1	2	172	13	0.86	167.9	2.7	96.6
Min	2	1	136	12	0.87	164.8	1.7	97.0
Min	2	2	167	12	0.94	165.4	2.3	97.6
Min	3	1	180	13	0.86	171.5	2.8	99.2
Min	3	2	149	14	0.85	173.3	2.7	97.0

B. CHEAM3 validation

intra-plate controls

Signal	Day	Plate	S:N	S:B	Z '	Avg Signal (RFU)	% CV	% growth
Max	1	1	169	12	0.89	14.6	6.5	0.0
Max	1	2	161	12	0.87	14.8	6.5	0.1
Max	2	1	200	11	0.79	14.8	6.0	-0.3
Max	2	2	186	11	0.70	15.0	6.1	-0.4
Max	3	1	273	11	0.90	15.1	6.2	-0.1
Max	3	2	175	11	0.88	15.1	6.4	-0.2
Mid	1	1	245	12	0.88	127.2	4.5	63.4
Mid	1	2	172	12	0.79	128.2	5.3	63.9
Mid	2	1	167	10	0.80	145.1	5.0	90.7
Mid	2	2	177	10	0.75	144.9	5.6	90.5
Mid	3	1	150	11	0.91	131.1	7.7	77.3

Mid	3	2	247	10	0.90	122.5	12.3	68.1
Min	1	1	237	12	0.93	183.3	2.8	100.4
Min	1	2	206	12	0.86	183.1	2.5	99.7
Min	2	1	130	10	0.78	145.9	6.1	98.3
Min	2	2	137	10	0.75	147.6	3.7	101.2
Min	3	1	187	11	0.88	165.7	2.7	98.2
Min	3	2	249	11	0.88	166.6	2.5	97.6

The Z' factor, an indication of the robustness of the assay (34) was ≥ 0.7 in all plates. S:N was > 100 for both strains and S:B was ≥ 12 for *Ds*Red and ≥ 10 for mCherry. The CV was < 20% in all plate. The average mid-point signal did not vary more than 1.5-fold within a run or across the three runs. Thus, both assays passed statistical validation.

High throughput screen

To examine the performance of our high-throughput assay, we tested a set of compounds with known activity against *M. tuberculosis*. The Tuberculosis Antimicrobial Acquisition and Coordinating Facility (TAACF) at the Southern Research Institute (SRI) screened libraries containing over 300,000 compounds to identify inhibitors of *M. tuberculosis* growth (35, 36). From the hits identified in these two screens a diversity set of 1105 compounds was made obtained from the Division of Microbiology and Infectious Disease (DMID), National Institute of Allergy and Infectious Diseases (NIAID.as a library of potential anti-tubercular agents for the further development of *M. tuberculosis* drug development assays (37). We obtained this set of compounds and tested them in both HTS-validated assays.

Compounds were obtained in plates, diluted to 0.35 mg/mL and transferred directly into assay plates to yield a final assay concentration of 7 µg/mL (final concentration of 2% DMSO). The standard assay conditions were used for each strain and % growth inhibition was plotted (Fig 4A and B). The Pearson coefficient, a statistical measurement of correlation between two data sets, was calculated for each strain. Fig 4A shows the replicate runs of CHEAM3 with a Pearson coefficient of r= 0.9843. When DREAM8 was the strain used in the screen the correlation coefficient was r= 0.9855 (Fig 4B). Thus the assay performed well in repeat runs with a large compound set.

Fig 4. Small molecule compound library screen: A selected library of 1105 small molecules from NIH-SRI/TAACF was screened in replicate experiments against **(A)** CHEAM3 or **(B)** DREAM8. The % inhibition for each compound was calculated. The results from the first and second runs are plotted on the x- and y-axis, respectively, for both strains. For each strain the Pearson coefficient of linear correlation between the two replicate data sets was calculated in Graphpad Prism and is shown in boxed text in the upper right corner of each plot. **(C)** Compounds' average % inhibition of CHEAM3 and DREAM8 growth was calculated and plotted on the x- and y- axis, respectively. The calculated Pearson co-efficient comparing the data generated from the two different strains is shown in boxed text in the upper right corner of the plot.

We compared the data between the two strains of *M. tuberculosis* strains (Fig 4C). There was a linear relationship between the two strains with a Pearson coefficient of r= 0.9074. Thus, there was no statistical difference between the two strains.

Using CHEAM3, 470 compounds inhibited *M. tuberculosis* growth ≥ 80% while 169 compounds inhibited ≥ 99% (Fig 4A). Using DREAM8, 403 compounds inhibited ≥ 80% growth and 182 compounds inhibited ≥ 99% growth (Fig 4B). 377 compounds inhibited ≥ 80% growth in both strains. There were some minor differences between the two strains. 141 compounds showed ≥ 99% inhibition in both strains, with an additional 69 compounds with %I ≥ 99 in only one of the two strains (41 in DREAM8 and 28 in CHEAM3). However, of these 69 compounds 64 inhibited growth of the alternate strain by at least 90%. The hits from the screen were analysed and revealed three chemotypes shown in Fig 5 that looked most interesting for further development: the phenoxyalkylbenzimidazoles (PAB), the benzothiophene 1-1 dioxides (BTD), and the piperidinamines (PIP).

Fig 5. Selected hit compounds from screen: Three hit chemotypes identified in our screen were noted as being especially interesting for further development. Their structures and MICs are shown.

DISCUSSION

We developed high throughput assays capable of screening large numbers of compounds using two fluorescent reporter strains of *M. tuberculosis*. We used both assays to screen a set of known compounds. Results from these assays were reproducible and the two strains yielded comparable results.

Only a fraction of the compounds we tested had activity against *M. tuberculosis* in our assays, even though these had previously been identified as active (35, 36). A significant

283 difference between the two screens is that we used a lower concentration of 7 µg/mL, as
284 compared to 20 µg/ml previously used; thus we will only detect the more potent
285 compounds. There are also some technical differences between the two assays, in
286 particular that we used OD_{590} and fluorescence as a measure of increase in bacterial
287 numbers, whereas the previous screen used Alamar Blue which monitors metabolic
288 activity.
289
290 Using our fluorescent reporter strains, we identified 210 compounds that inhibited ≥ 99%
291 growth, 141 of which inhibited ≥ 99% growth in both strains. We highlighted three
292 chemotypes that were most interesting as the phenoxyalkylbenzimidazoles (PAB),
293 benzothiophene 1-1 dioxides (BTD), and piperidinamines (PIP). We selected these
294 chemical classes as being novel anti-mycobacterials and we (and others) have
295 investigated these further in other publications pertaining to their recent characterization
296 and development.
297
298 Compounds containing the benzimidazole core have long been known to have broad
299 spectrum antibacterial activity (38, 39). In the *M. tuberculosis* phenotypic screen
300 performed by Ananthan et al., 88 compounds with the phenoxyalkylimidazole core were
301 tested, PAB being the most potent active identified in this series, and the only compound
302 in that study with benzimidazole substituted for the imidazole (35). There have since been
303 reports of benzimidazoles having activity against *M. tuberculosis* (40, 41). We
304 investigated this series and confirmed its potent activity and selectivity (42). We have also

shown that this class of compounds targets the electron transport chain, specifically targeting QcrB (43).

The benzothiophene 1-1 dioxides (BTD) series was also highlighted by Ananthan et al., as a chemotype. There were only a small number of analogs within this chemotype in their larger screen, all containing a thioether group at the 3-position and the most potent being the compound shown in Fig 5. They further noted that there were 40 additional compounds with the thiopene 1-1 dioxides lacking the benzene substitution in their primary screen, all of which lacked activity. Using this as a starting point we explored the BTD series and evaluated their activity against *M. tuberculosis*. We were able to derive compounds that had good anti-tubercular activity (with MICs of 3-8 μM) but were unable to identify potent compounds analogs that were not cytotoxic to eukaryotic cells (44).

Some work has been done on piperidinamine-containing molecules as motilin-receptor agonists (45) and their clinical development for treating type 1 diabetes (46, 47). Our screen identified the piperidinamines (PIP) as a potent chemotype. We obtained analogs within this chemotype that were commercially available and evaluated them for activity against *M. tuberculosis*, but none showed activity (48). Based on our exploration of modifications around the piperidine core, we were unable to identify avenues for improved activity, and to our knowledge, the PIP chemotype has not yet further developed as an anti-tubercular agent.

In summary, we have developed and validated a robust whole cell phenotypic assay for *M. tuberculosis* in 384-well plates using one of two fluorescent reporters with equivalent outcomes. We used these assays to identify potent inhibitors of *M. tuberculosis* growth that have since proven to be interesting leads for drug development. This assay provides robust and reproducible results, and can be a core tool for high-throughput screening of large chemical libraries for the discovery of novel chemical entities to treat tuberculosis

Acknowledgements

None

References

1. World Health Organization. Global tuberculosis report 2017.

2. Galandrin S, Guillet V, Rane RS, Leger M, N R, Eynard N, et al. Assay development for identifying inhibitors of the mycobacterial FadD32 activity. J Biomolec Screen. 2013;18(5):576-87.

3. Geist JG, Lauw S, Illarionova V, Illarionov B, Fischer M, Grawert T, et al. Thiazolopyrimidine inhibitors of 2-methylerythritol 2,4-cyclodiphosphate synthase (IspF) from *Mycobacterium tuberculosis* and *Plasmodium falciparum*. ChemMedChem. 2010;5(7):1092-101.

4. Humnabadkar V, Jha RK, Ghatnekar N, De Sousa SM. A high-throughput screening assay for simultaneous selection of inhibitors of *Mycobacterium tuberculosis* 1-deoxy-D-xylulose-5-phosphate synthase (Dxs) or 1-deoxy-D-xylulose 5-phosphate reductoisomerase (Dxr). J Biomolec Screen. 2011;16(3):303-12.

5. Kumar A, Casey A, Odingo J, Kesicki EA, Abrahams G, Vieth M, et al. A high-throughput screen against pantothenate synthetase (PanC) identifies 3-biphenyl-4-cyanopyrrole-2-carboxylic acids as a new class of inhibitor with activity against *Mycobacterium tuberculosis*. PLOS One. 2013;8(11):e72786.

6. Mann S, Eveleigh L, Lequin O, Ploux O. A microplate fluorescence assay for DAPA aminotransferase by detection of the vicinal diamine 7,8-diaminopelargonic acid. Anal Biochem. 2013;432(2):90-6.

7. Simithy J, Reeve N, Hobrath JV, Reynolds RC, Calderon AI. Identification of shikimate kinase inhibitors among anti-*Mycobacterium tuberculosis* compounds by LC-MS. Tuberculosis. 2014;94(2):152-8.

8. Anthony KG, Strych U, Yeung KR, Shoen CS, Perez O, Krause KL, et al. New classes of alanine racemase inhibitors identified by high-throughput screening show antimicrobial activity against *Mycobacterium tuberculosis*. PLOS One. 2011;6(5):e20374.

9. Bhat J, Rane R, Solapure SM, Sarkar D, Sharma U, Harish MN, et al. High-throughput screening of RNA polymerase inhibitors using a fluorescent UTP analog. J Biomolec Screen. 2006;11(8):968-76.

10. Gutierrez-Lugo MT, Baker H, Shiloach J, Boshoff H, Bewley CA. Dequalinium, a new inhibitor of *Mycobacterium tuberculosis* mycothiol ligase identified by high-throughput screening. Journal of biomolecular screening. 2009;14(6):643-52.

11. Sha S, Zhou Y, Xin Y, Ma Y. Development of a colorimetric assay and kinetic analysis for *Mycobacterium tuberculosis* D-glucose-1-phosphate thymidylyltransferase. J Biomolec Screen.. 2012;17(2):252-7.

12. Singh U, Sarkar D. Development of a simple high-throughput screening protocol based on biosynthetic activity of *Mycobacterium tuberculosis* glutamine synthetase for the identification of novel Inhibitors. J Biomolec Screen.. 2006;11(8):1035-42.

13. White EL, Southworth K, Ross L, Cooley S, Gill RB, Sosa MI, et al. A novel inhibitor of *Mycobacterium tuberculosis* pantothenate synthetase. J Biomolec Screen.. 2007;12(1):100-5.

14. Zhao N, Darby CM, Small J, Bachovchin DA, Jiang X, Burns-Huang KE, et al. Target-based screen against a periplasmic serine protease that regulates intrabacterial pH homeostasis in *Mycobacterium tuberculosis*. ACS Chem Biol. 2015;10(2):364-71.

15. Santa Maria JP, Jr., Park Y, Yang L, Murgolo N, Altman MD, Zuck P, et al. Linking high-throughput screens to identify MOAs and novel inhibitors of *Mycobacterium tuberculosis* dihydrofolate reductase. ACS Chem Biol. 2017;12(9):2448-56.

16. Payne DJ, Gwynn MN, Holmes DJ, Pompliano DL. Drugs for bad bugs: confronting the challenges of antibacterial discovery. Nature Rev Drug Disc. 2007;6(1):29-40.

17. Gholap S, Tambe M, Nawale L, Sarkar D, Sangshetti J, Damale M. Design, synthesis, and pharmacological evaluation of fluorinated azoles as anti-tubercular agents. Archiv der Pharmazie. 2018;351(2).

386 18. Cheng N, Porter MA, Frick LW, Nguyen Y, Hayden JD, Young EF, et al. Filtration improves
387 the performance of a high-throughput screen for anti-mycobacterial compounds. PLOS One.
388 2014;9(5):e96348.
389 19. Chung GA, Aktar Z, Jackson S, Duncan K. High-throughput screen for detecting
390 antimycobacterial agents. Antimicrob Ag Chemother. 1995;39(10):2235-8.
391 20. Grant SS, Kawate T, Nag PP, Silvis MR, Gordon K, Stanley SA, et al. Identification of
392 novel inhibitors of nonreplicating *Mycobacterium tuberculosis* using a carbon starvation model.
393 ACS Chem Biol. 2013;8(10):2224-34.
394 21. Deb C, Lee CM, Dubey VS, Daniel J, Abomoelak B, Sirakova TD, et al. A novel in vitro
395 multiple-stress dormancy model for *Mycobacterium tuberculosis* generates a lipid-loaded, drug-
396 tolerant, dormant pathogen. PLOS One. 2009;4(6):e6077.
397 22. Gold B, Pingle M, Brickner SJ, Shah N, Roberts J, Rundell M, et al. Nonsteroidal anti-
398 inflammatory drug sensitizes *Mycobacterium tuberculosis* to endogenous and exogenous
399 antimicrobials. Proc Natl Acad Sci U S A. 2012;109(40):16004-11.
400 23. Brodin P, Poquet Y, Levillain F, Peguillet I, Larrouy-Maumus G, Gilleron M, et al. High
401 content phenotypic cell-based visual screen identifies *Mycobacterium tuberculosis* acyltrehalose-
402 containing glycolipids involved in phagosome remodeling. PLoS Pathogens. 2010;6(9):e1001100.
403 24. Christophe T, Ewann F, Jeon HK, Cechetto J, Brodin P. High-content imaging of
404 *Mycobacterium tuberculosis*-infected macrophages: an in vitro model for tuberculosis drug
405 discovery. Future Med Chem. 2010;2(8):1283-93.
406 25. Mak PA, Rao SP, Ping Tan M, Lin X, Chyba J, Tay J, et al. A high-throughput screen to
407 identify inhibitors of ATP homeostasis in non-replicating *Mycobacterium tuberculosis*. ACS Chem
408 Biol. 2012;7(7):1190-7.
409 26. Darby CM, Ingolfsson HI, Jiang X, Shen C, Sun M, Zhao N, et al. Whole cell screen for
410 inhibitors of pH homeostasis in *Mycobacterium tuberculosis*. PLOS One. 2013;8(7):e68942.

411 27. Wang F, Sambandan D, Halder R, Wang J, Batt SM, Weinrick B, et al. Identification of a
412 small molecule with activity against drug-resistant and persistent tuberculosis. Proc Natl Acad Sci
413 U S A. 2013;110(27):E2510-7.
414 28. Cho SH, Warit S, Wan B, Hwang CH, Pauli GF, Franzblau SG. Low-oxygen-recovery
415 assay for high-throughput screening of compounds against nonreplicating *Mycobacterium*
416 *tuberculosis*. Antimicrob Ag Chemother. 2007;51(4):1380-5.
417 29. Ioerger TR, Feng Y, Ganesula K, Chen X, Dobos KM, Fortune S, et al. Variation among
418 genome sequences of H37Rv strains of *Mycobacterium tuberculosis* from multiple laboratories. J
419 Bacteriol. 2010;192(14):3645-53.
420 30. Carroll P, Schreuder LJ, Muwanguzi-Karugaba J, Wiles S, Robertson BD, Ripoll J, et al.
421 Sensitive detection of gene expression in mycobacteria under replicating and non-replicating
422 conditions using optimized far-red reporters. PLOS One. 2010;5(3):e9823.
423 31. Carroll P, Muwanguzi J, Parish T. Optimization of the DsRed fluorescent protein for use
424 in *Mycobacterium tuberculosis*. bioRxiv. 2018. https://doi.org/10.1101/383836
425 32. Ollinger J, Bailey MA, Moraski GC, Casey A, Florio S, Alling T, et al. A dual read-out assay
426 to evaluate the potency of compounds active against *Mycobacterium tuberculosis*. PLOS One.
427 2013;8(4):e60531.
428 33. Iversen PW, Beck B, Chen Y-F, Dere W, Devanarayan V, Eastwood BJ, et al. HTS Assay
429 Validation. 2012. In: Assay Guidance Manual [Internet]. Eli Lilly & Company and the National
430 Center for Advancing Translational Sciences. Available from:
431 https://www.ncbi.nlm.nih.gov/books/NBK83783/.
432 34. Zhang JH, Chung TD, Oldenburg KR. A simple statistical parameter for use in evaluation
433 and validation of high throughput screening assays. J Biomolec Screen. 1999;4(2):67-73.
434 35. Ananthan S, Faaleolea ER, Goldman RC, Hobrath JV, Kwong CD, Laughon BE, et al.
435 High-throughput screening for inhibitors of *Mycobacterium tuberculosis* H37Rv. Tuberculosis.
436 2009;89(5):334-53.

437 36. Maddry JA, Ananthan S, Goldman RC, Hobrath JV, Kwong CD, Maddox C, et al.
438 Antituberculosis activity of the molecular libraries screening center network library. Tuberculosis
439 . 2009;89(5):354-63.
440 37. Goldman RC, Laughon BE. Discovery and validation of new antitubercular compounds as
441 potential drug leads and probes. Tuberculosis. 2009;89(5):331-3.
442 38. He Y, Wu B, Yang J, Robinson D, Risen L, Ranken R, et al. 2-piperidin-4-yl-
443 benzimidazoles with broad spectrum antibacterial activities. Bioorg Med Chem Lett.
444 2003;13(19):3253-6.
445 39. Ozkay Y, Tunali Y, Karaca H, Isikdag I. Antimicrobial activity and a SAR study of some
446 novel benzimidazole derivatives bearing hydrazone moiety. Eur J Med Chem. 2010;45(8):3293-
447 8.
448 40. Ojima I, Kumar K, Awasthi D, Vineberg JG. Drug discovery targeting cell division proteins,
449 microtubules and FtsZ. Bioorg Med Chem. 2014;22(18):5060-77.
450 41. Gong Y, Somersan Karakaya S, Guo X, Zheng P, Gold B, Ma Y, et al. Benzimidazole-
451 based compounds kill *Mycobacterium tuberculosis*. Eur J Med Chem. 2014;75:336-53.
452 42. Chandrasekera NS, Alling T, Bailey MA, Files M, Early JV, Ollinger J, et al. Identification
453 of Phenoxyalkylbenzimidazoles with Antitubercular Activity. J Med Chem. 2015;58(18):7273-85.
454 43. Chandrasekera NS, Berube BJ, Shetye G, Chettiar S, O'Malley T, Manning A, et al.
455 Improved phenoxyalkylbenzimidazoles with activity against *Mycobacterium tuberculosis* appear
456 to target QcrB. ACS Infect Dis. 2017;3(12):898-916.
457 44. Chandrasekera NS, Bailey MA, Files M, Alling T, Florio SK, Ollinger J, et al. Synthesis
458 and anti-tubercular activity of 3-substituted benzo[b]thiophene-1,1-dioxides. PeerJ. 2014;2:e612.
459 45. Westaway SM, Brown SL, Fell SC, Johnson CN, MacPherson DT, Mitchell DJ, et al.
460 Discovery of N-(3-fluorophenyl)-1-[(4-([(3S)-3-methyl-1-piperazinyl]methyl)phenyl)acetyl]-4-pi
461 peridinamine (GSK962040), the first small molecule motilin receptor agonist clinical candidate. J
462 Med Chem. 2009;52(4):1180-9.

463 46. Chapman MJ, Deane AM, O'Connor SL, Nguyen NQ, Fraser RJ, Richards DB, et al. The
464 effect of camicinal (GSK962040), a motilin agonist, on gastric emptying and glucose absorption
465 in feed-intolerant critically ill patients: a randomized, blinded, placebo-controlled, clinical trial. Crit
466 Care. 2016;20(1):232.
467 47. Hellstrom PM, Tack J, Johnson LV, Hacquoil K, Barton ME, Richards DB, et al. The
468 pharmacodynamics, safety and pharmacokinetics of single doses of the motilin agonist, camicinal,
469 in type 1 diabetes mellitus with slow gastric emptying. Br J Pharmacol. 2016;173(11):1768-77.
470 48. Chandrasekera NS, Alling T, Bailey M, Korkegian A, Ahn J, Ovechkina Y, et al. The 4-
471 aminopiperidine series has limited anti-tubercular and anti-staphylococcus aureus activity. J
472 Negat Results Biomed. 2015;14:4.

473

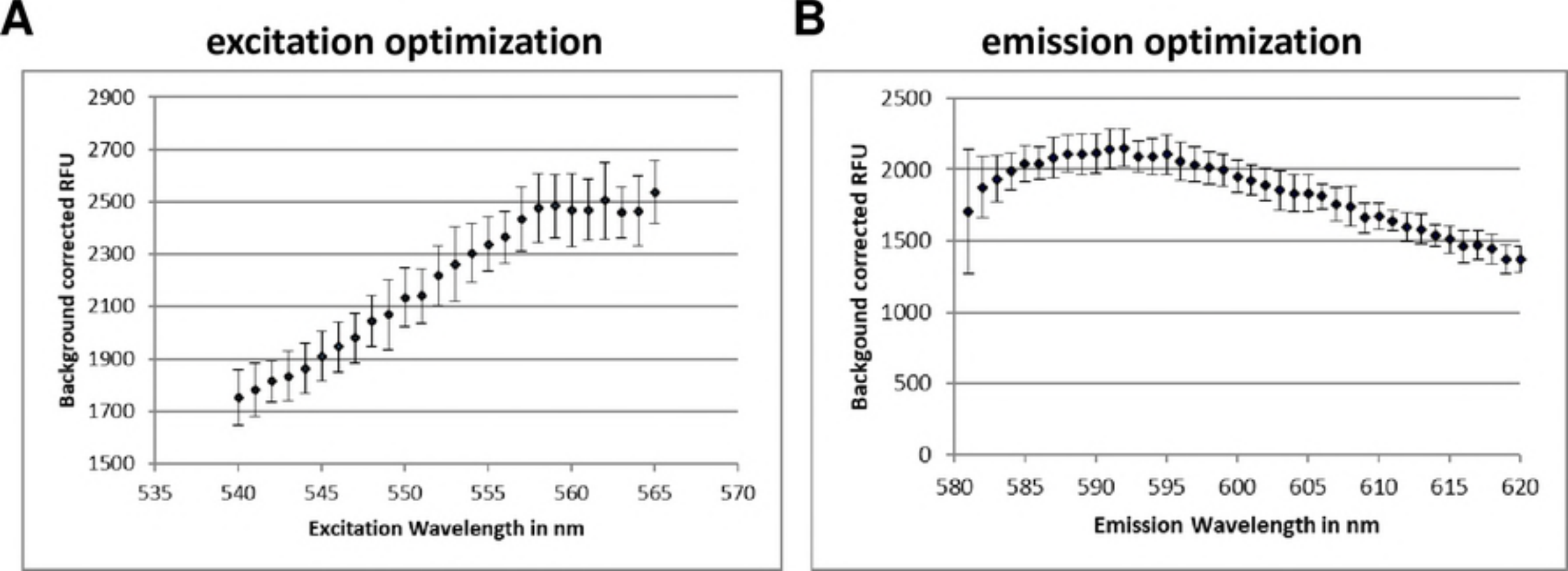
A
excitation optimization
Background corrected RFU
2900
2700
2500
2300
2100
1900
1700
1500
535
540
545
550
555
560
565
570
Excitation Wavelength in nm
B
emission optimization
Backgound corrected RFU
2500
2000
1500
1000
500
0
580
585
590
595
600
605
610
615
620
Emission Wavelength in nm

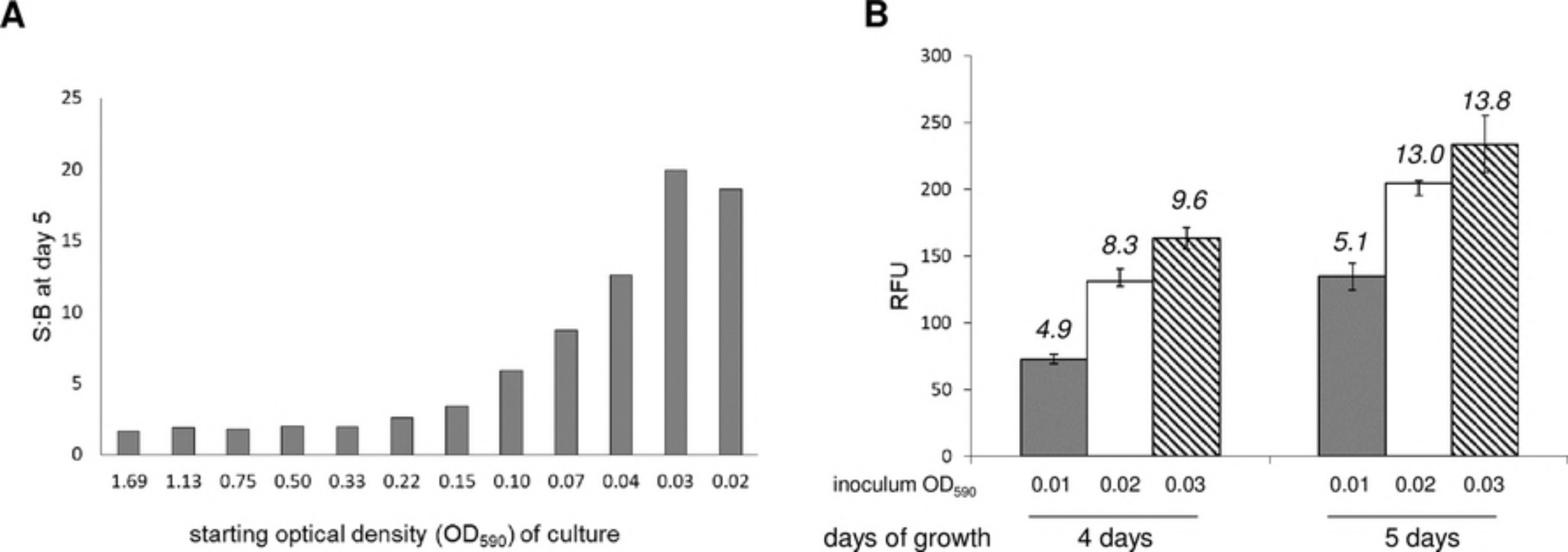
A
S:B at day 5
25
20
15
10
5
0
1.69 1.13 0.75 0.50 0.33 0.22 0.15 0.10 0.07 0.04 0.03 0.02
starting optical density (OD590) of culture
B
RFU
300
250
200
150
100
50
0
4.9
8.3
9.6
5.1
13.0
13.8
inoculum OD590
0.01 0.02 0.03
0.01 0.02 0.03
days of growth
4 days
5 days

A

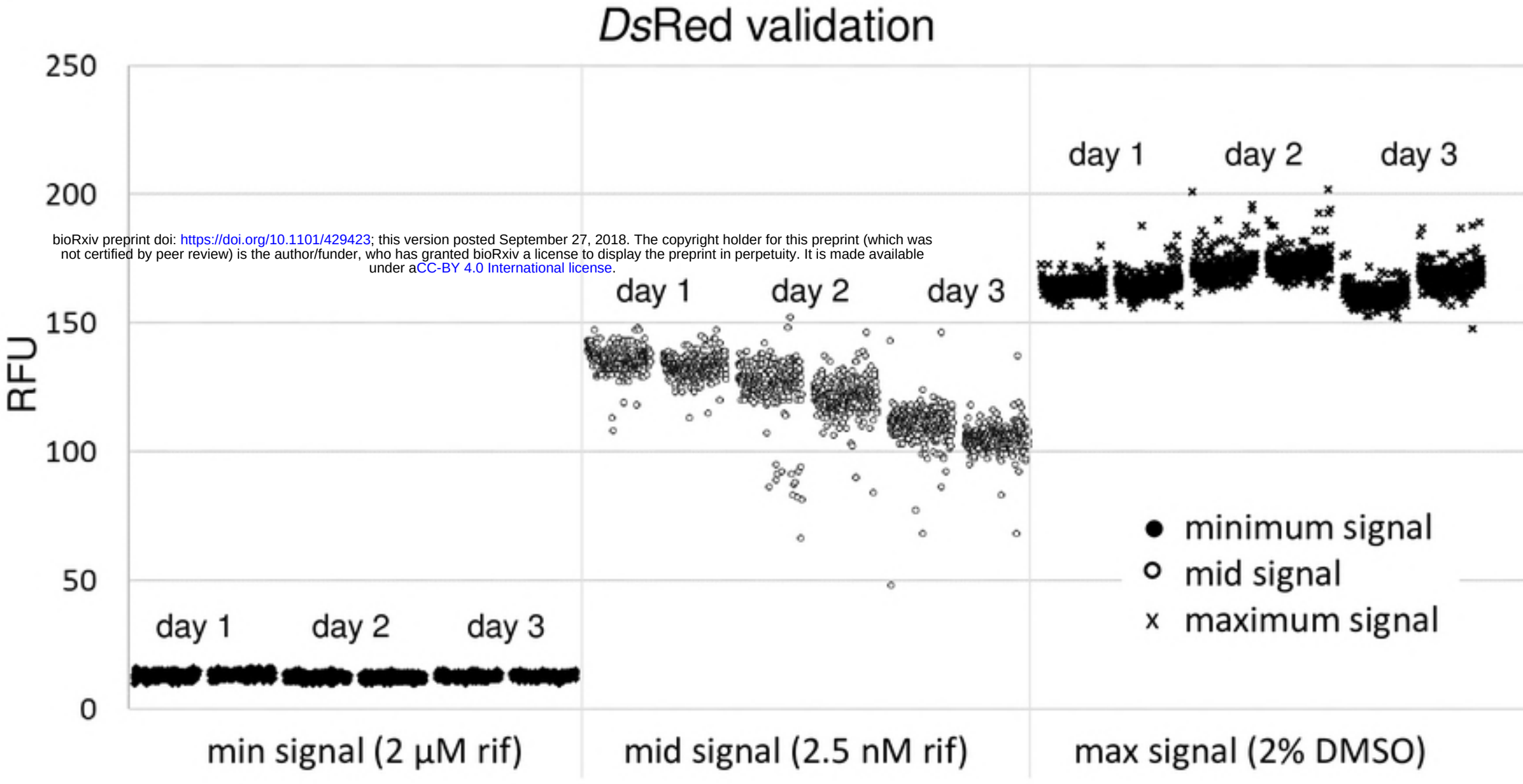

B

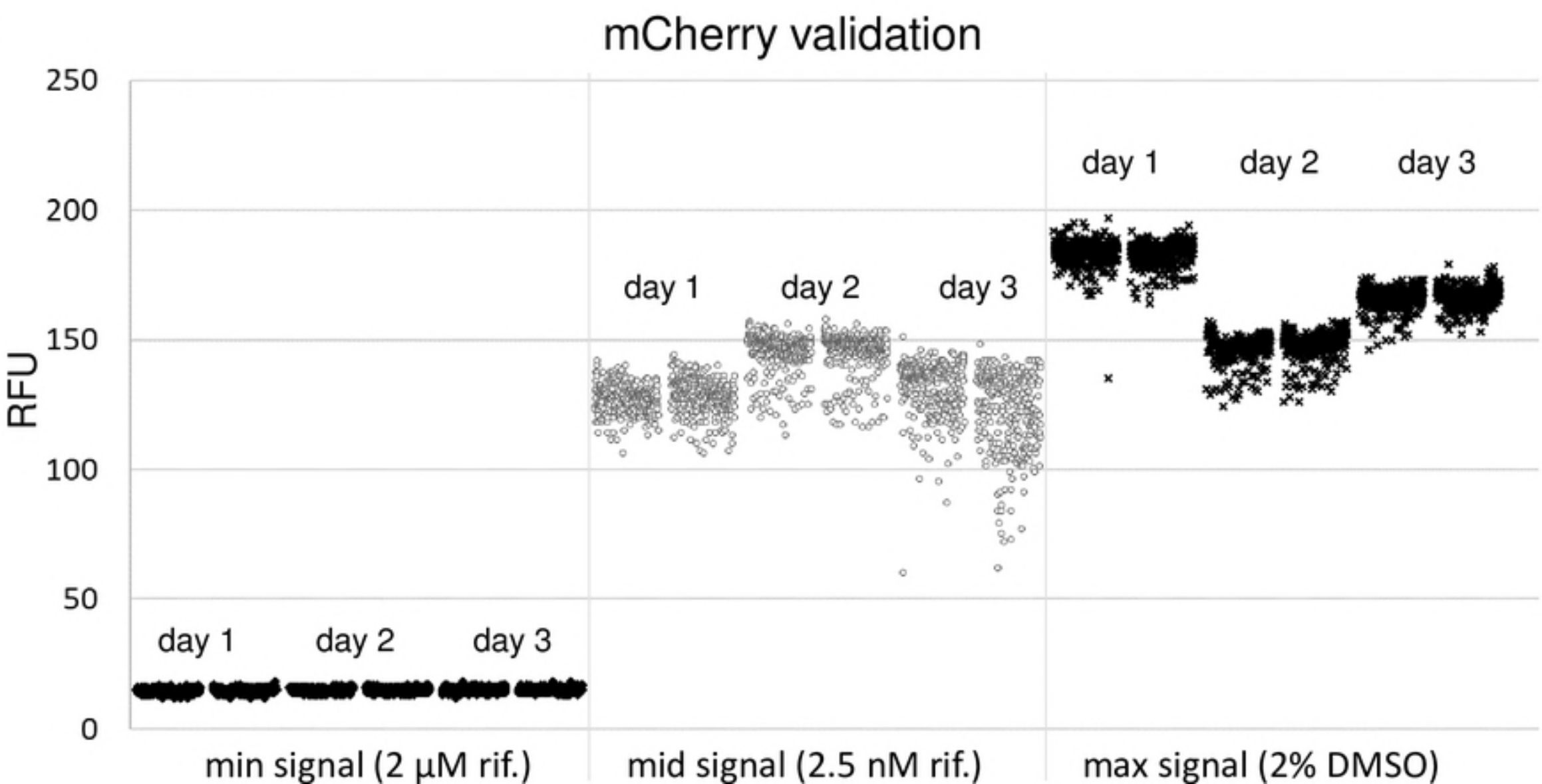

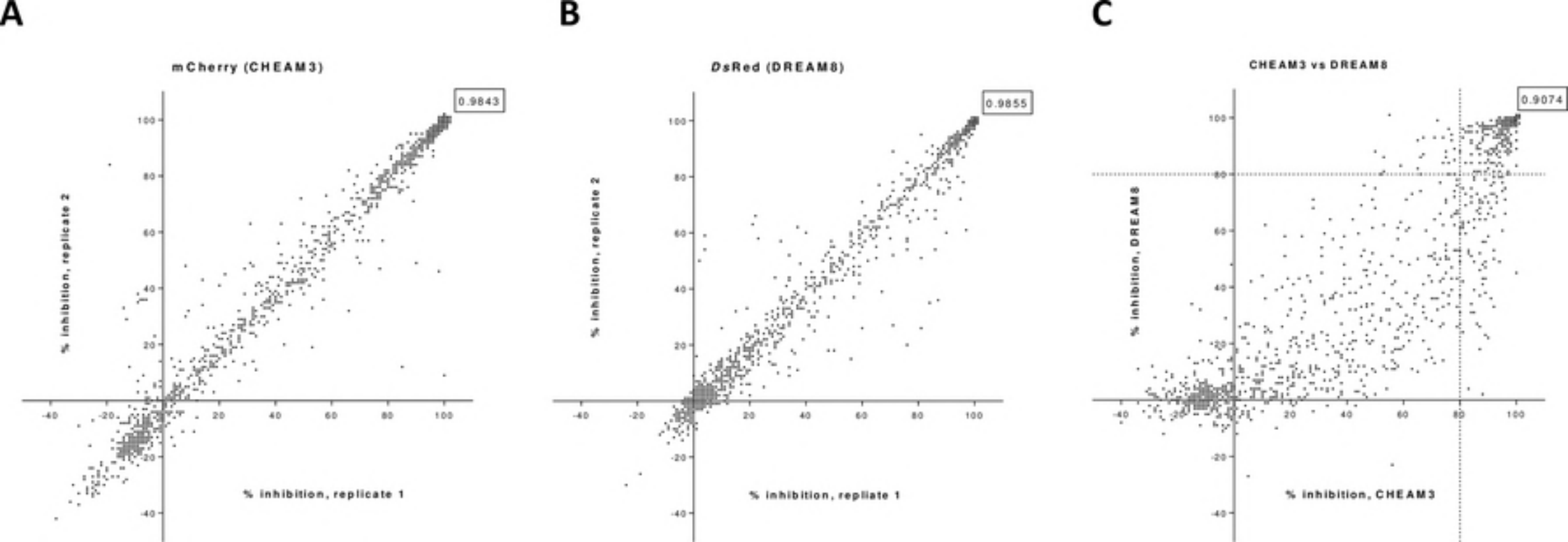
A
mCherry (CHEAM3)
0.9843
% inhibition, replicate 2
% inhibition, replicate 1
B
DsRed (DREAM8)
0.9855
% inhibition, replicate 2
% inhibition, repliate 1
C
CHEAM3 vs DREAM8
0.9074
% inhibition, DREAM8
% inhibition, CHEAM3

phenoxyalkylbenzimidazole (**PAB**)
MIC = 5.2 ± 1.5 µM (n=4)

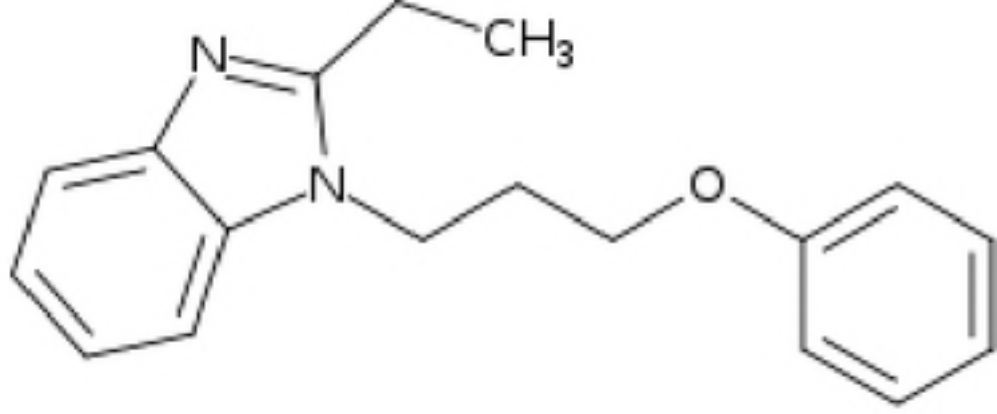

benzothiophene-1,1-dioxide (**BTD**)
MIC = 3.1 ± 0.07 µM (n=2)

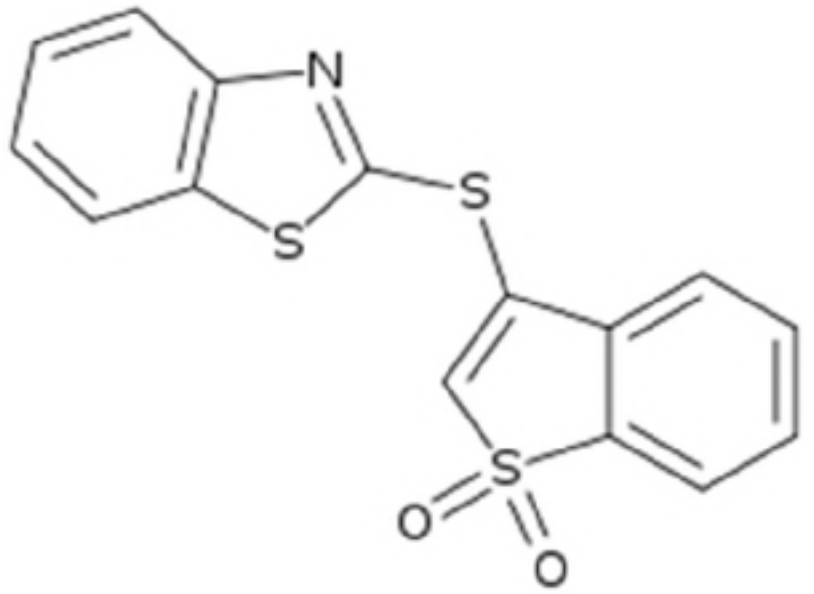

piperidinamine (**PIP**)
MIC = 9.9 ± 0.2 µM (n=2)